

Effect of Relative Humidity on Oxidation of Flaxseed Oil in Spray Dried Whey Protein Emulsions

RIITTA PARTANEN,^{*,†} JANNE RAULA,[‡] RAUNI SEPPÄNEN,[§] JOHANNA BUCHERT,[†]
 ESKO KAUPPINEN,^{†,‡} AND PIIRKKO FORSSELL[†]

VTT Technical Research Centre of Finland, Espoo, Finland; NanoMaterials Group, Laboratory of Physics and Center for New Materials, Helsinki University of Technology, Espoo, Finland; and YKI, Institute for Surface Chemistry, Stockholm, Sweden

Flaxseed oil was emulsified in whey protein isolate (WPI) and spray-dried. Powder characteristics and oxidative stability of oil at relative humidities (RH) from RH ~0% to RH 91% at 37 °C were analyzed. Oil droplets retained their forms in drying and reconstitution, but the original droplet size of the emulsion was not restored when the powder was dispersed in water. The particles seemed to be covered by a protein-rich surface layer as analyzed by electron spectroscopy for chemical analysis (ESCA). Oxidation of flaxseed oil dispersed in the WPI matrix was retarded from that of bulk oil but followed the same pattern as bulk oil with respect to humidity. A high rate of oxidation was found for both low and high humidity conditions. The lowest rate of oxidation as followed by peroxide values was found at RH 75%, a condition that is likely to diverge significantly from the monolayer moisture value. A weak baseline transition observed for the WPI matrix in a differential scanning calorimetry (DSC) thermogram suggested a glassy state of the matrix at all storage conditions. This was not consistent with the observed caking of the powder at RH 91%. Scanning electron microscopy (SEM) images revealed a considerable structural change in the WPI matrix in these conditions, which was suggested to be linked with a higher rate of oxygen transport. Possible mechanisms for oxygen transport in the whey protein matrix under variable RHs are discussed.

KEYWORDS: Whey protein isolate; WPI; oxidation; relative humidity; flaxseed oil; oxidative stability

INTRODUCTION

Lipid oxidation leads to off-flavor formation in foods (1). Controlling these reactions is especially important when highly unstable polyunsaturated fatty acids are involved. In bulk fats and oils, oxidation mechanisms are fairly well-known, but oxidation in the dispersed lipid phase is further complicated by structurally and compositionally heterogeneous matrices (2).

Oxygen is a requirement for oxidation and formation of primary oxidation products from unsaturated fatty acids (i.e., fatty acid hydroperoxides). In a solid, glassy matrix, oxygen transport may be limited by solubility and diffusion of oxygen in the matrix, both of which are influenced by the amount of water present in carbohydrate glasses (3). Carbohydrates are good barriers for oxygen at low humidity. As they are plasticized by water with increasing humidity, the barrier properties are lost (4, 5). Results of dispersed lipid in a carbohydrate-rich matrix indicate the importance of the physical state of the matrix on oxidation rate (6–8).

Proteins being less hydrophilic than carbohydrates have been widely studied in stabilizing food emulsions. In dried emulsions, proteins have been mostly studied in combination with carbohydrates (9–12). Thus, relatively little information exists on the effect of water on oxidation in matrices made of only proteins. Systems with both proteins and carbohydrates are complicated by the possible formation of Maillard reaction products (10) and low humidity tolerance of most carbohydrates. Because of the collapse of these powders at high humidity, the data on oxidative stability of matrix dispersed oil at high humidity conditions is scarce. There is also a lack of data on oxygen permeation of whey protein matrices, although barrier properties of plasticized whey protein films have been studied extensively by Krochta and co-workers (13–16). Moreau and Rosenberg have studied the oxidation of milk fat (17) and porosity and gas permeation (18) in similar spray-dried whey-protein particles. It was concluded that, even if the matrix was permeable to gases, the lipid was sealed from gas permeation most likely due to a dense interfacial layer. A very recent study on oxygen permeability in amorphous β -lactoglobulin films suggested that increase in oxygen permeation reflected the softening in the protein matrix with transition from a glassy to rubbery state (19).

The aim of this work was to elucidate the role of the protein matrix in controlling oxidation of oil emulsified in whey protein

* To whom correspondence should be addressed. Phone: +358 40 825 5816. Fax: +358 20 722 7071. E-mail: riitta.partanen@vtt.fi.

[†] VTT Technical Research Centre of Finland.

[‡] Helsinki University of Technology.

[§] Institute for Surface Chemistry.

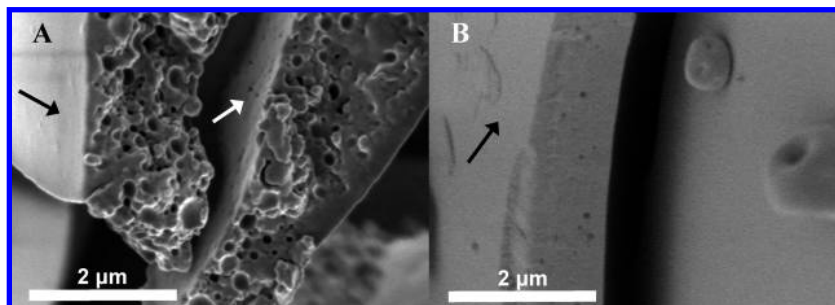


Figure 1. Cross-section images of powder particles of (A) WPI-FSO emulsion and (B) WPI reference (without oil) after drying. Outer surfaces are indicated by black arrows; inner surface is indicated by white arrow.

isolate and the effect of water activity on the rate of oxidation. Thus, the potential of whey protein isolate in retarding oil oxidation at low ($a_w \sim 0$ and 0.1), intermediate (a_w 0.49), and high (a_w 0.75 and 0.91) a_w was studied using bulk oil oxidation as a reference. The influence of sorbed water on the protein matrix and on lipid oxidation rate is discussed.

MATERIALS AND METHODS

Materials. Flaxseed oil was a product of Elixii oil Oy (Somero, Finland), where the fatty acid content was the following (4% 16:0, 3% 18:0, 12% 18:1, 15% 18:2, 66% 18:3). Whey protein isolate (Lacprodan, Arla Foods Ingredients, Viby J, Denmark) was essentially free of lactose (max. 0.5%) and had a minimum protein content of 91% (of dry weight). All other reagents were of analytical grade.

Emulsification of Oil. Whey protein isolate (WPI) was dissolved in water (10 wt %, pH 7) at room temperature. Sodium azide (0.04 wt %) was added as a preservative. The solution was prehomogenized with flaxseed oil (40% oil of the dry weight of the sample for spray-drying) with a Heidolph Diax 900 (Heidolph Instruments GmbH and Co KG, Schwabach, Germany) homogenizer at 26 000 rpm for 2 × 2 min. Pre-emulsion was fed to the pressure homogenizer M-110Y (Microfluidics, Newton, MA) and circulated for 10 min at 40 psig.

Spray Drying of Emulsions. Emulsions were spray-dried by a laboratory spray-drier Niro Mobile Minor (Niro A/S, Soeborg, Denmark) with a cocurrent two-fluid nozzle. The inlet air temperature was adjusted to 180 °C, and the outlet temperature was kept at 90 ± 3 °C by controlling the flow rate. The atomization pressure was 1 bar, and the pressurized air consumption was 7 kg/h. Samples were collected in the chamber and cyclone collection vessels.

Droplet Size Distribution. Oil droplet size distribution in emulsions was analyzed by laser diffraction with Coulter LS 230 (Beckman Coulter, Fullerton, CA) equipped with polarization intensity differential scattering (PIDS) assembly for particles smaller than 0.4 μm. Results were calculated using an optical model, where the droplets were assumed to be spherical in shape with a refractive index of 1.6. Duplicate measurements were performed.

Glass Transition Temperature. Glass transition temperature was determined by differential scanning calorimetry (DSC) with Mettler Toledo DSC820 (Dietikon, Switzerland) equipped with a liquid nitrogen cooling system. A sample of approximately 10 mg was weighed into a 40 μL aluminum sample pan, which was then sealed and measured at 10 °C/min heating/cooling rate. The temperature range measured was -20 °C to +100 °C in the first heating, 100 °C to -20 °C in cooling, and -20 °C to +130 °C in the second heating, from which glass transition was taken as the midpoint value. Duplicate measurements were performed.

Extraction of Oil for Peroxide Value Determination. The extraction was carried out by the method modified from Kellerby et al. (20). A powder sample of 0.5 g was weighed into a test tube and suspended in 5 mL of water. The tube was shaken for 30 min to ensure dissolution of the powder. A 300 μL portion was taken and vortexed 3 times for 10 s with 1.5 mL of an iso-octane/isopropanol (2:1) mixture to extract the oil. The phases were separated by centrifugation (1000g for 4 min). Longer times were applied if necessary. Triplicate extractions were performed.

Peroxide Value Determination. Peroxide value was determined spectrophotometrically according to IDF standard 74A:1991 (21). A portion of oil (0.1–0.3 g) was weighed or in the case of powders 200 μL of extraction medium was taken for analysis and added to 9.6 mL of a chloroform/methanol (7:3) mixture. For color formation, 50 μL of both iron(II) chloride and ammonium thiocyanate solutions were added. The sample was briefly vortexed, reacted in the dark for exactly 5 min, and measured at 500 nm. Triplicate measurements were performed, and standard deviations were calculated.

SEM Micrographs. The morphology of the particles was imaged with a field-emission scanning electron microscope, FE-SEM (Leo DSM982 Gemini, LEO Electron Microscopy Inc., Germany) with the operating voltage of 0.7 kV or 2.0 kV. To investigate the particle interior, some of the particles were fractured by the fast removal of sticky tape placed on the sample. Then, the samples were coated with sputtered platinum in order to stabilize them under the electron beam and to enhance image contrast.

Surface Composition. The surface chemical composition of oil was determined with a Kratos AXIS HS X-ray photoelectron spectrometer (Kratos Analytical, U.K.). By ESCA, it is possible to identify elements present on the surface of a specimen. Relative atomic concentrations can be quantified using appropriate sensitivity factors (supplied by Kratos Analytical, U.K.). Electrons emitted from the sample originate from the near-surface region for most solids (2–10 nm). The instrument used a monochromatic Al K_α X-ray source. The pressure in the vacuum chamber during the analysis was $< 10^{-10}$ bar. The takeoff angle of the photoelectrons was perpendicular to the sample. Analyses were made on an area of less than 1 mm². The atomic concentrations of carbon, oxygen, and nitrogen were determined. Duplicate measurements were performed. The elemental ratios of the sample were assumed to be a linear combination of the elemental ratios of the protein and oil making it up (22).

Storage Stability Test. Powder and oil samples were spread on Petri dishes and stored in closed chambers without light exposure under phosphorus pentoxide (~RH 0%) or supersaturated salt solutions (RH 11, 49, 75, 91%) at 37 °C. Statistical analysis for the end of storage test at 9 weeks was performed by paired *t* tests at the 95% confidence level using the SPSS software (SPSS 10.0, SPSS Inc.).

RESULTS AND DISCUSSION

Distribution of Oil in WPI Powders. Spray-dried flaxseed oil emulsion powder was prepared, and the wall structure was imaged by SEM using low voltage to protect the samples from any possible structural deterioration under the electron beam. Powder particles in the size of tens of microns resulted from drying. A cross-section image of the thin wall of an emulsion powder particle is presented in **Figure 1A**. To discriminate between oil droplets and porosity in the sample, WPI was spray-dried also without oil (**Figure 1B**). The powders differed considerably in appearance. Small spherical holes of the size of oil droplets (**Figure 2**) were observed in the cross cut of the emulsion powder particle. The inner surface of the particle resembled the porosity in the cross-cut surface of the WPI reference. Spray-dried particles are often

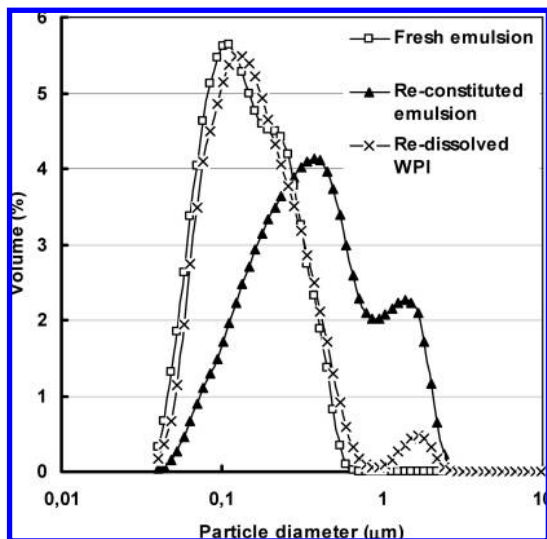


Figure 2. Particle size distributions of fresh and reconstituted spray-dried emulsions and spray-dried whey protein isolate suspended in water.

Table 1. Elemental Ratios of Carbon (C), Nitrogen (N), and Oxygen (O) in Whey Protein and Flaxseed Oil (Theoretical), as well as at the Outermost Surface of the Spray-Dried Whey Protein Isolate (WPI) Emulsion with 40 wt% Flaxseed Oil (FSO) Determined by ESCA^a

	C (wt%)	N (wt%)	O (wt%)
whey protein	65	16	19
flaxseed oil	88	0	12
spray-dried WPI–FSO emulsion	71	12	17

^a The atomic ratios were determined, and the weight ratios were calculated based on the atomic masses.

hollow spheres. Formation of the central void is related to vaporization of moisture (23).

A different, more homogeneous structure was observed close to the particle outer surface. The surface composition was more closely studied by ESCA, which is a surface-sensitive technique for elemental analysis. On the basis of the elemental ratios of carbon (C), nitrogen (N), and oxygen (O) determined by ESCA (Table 1), the oil content in the near-surface region was calculated assuming that the elemental ratios of the sample are a linear combination of the elemental ratios of the protein and the oil making it up (22). At the near-surface region, the oil content was estimated to be 26% as compared to 40% total oil content. Some of the electrons could be emitted from oil below the interfacial protein layer, which is expected to be very thin, only 3 nm in thickness (24). The result was interpreted as a protein-rich outer surface in the particles rather than an indication of nonemulsified surface oil. Enrichment of protein in the sample surface could also be evidenced simply by the N content. Somewhat different surface composition by ESCA in milk protein-stabilized emulsions was found by Millqvist-Fureby et al. (25). The powders containing 30% oil were found to have a fat coverage between 56 and 70%. In that study, the powder particles were considerably smaller as compared with particles of the present study, which may at least partially explain the observed difference.

The size distribution of the reconstituted emulsion measured by laser diffraction was changed from that of the original emulsion (Figure 2). The median particle size in the original emulsion was 0.14 μm and in the reconstituted emulsion 0.38 μm . Similar behavior has been reported for whey protein emulsions before (25, 26). Hogan et al. (26) found an increase in size distribution of the redispersed powder as the oil/protein ratio increased. In water, a more pronounced increase was observed, which was linked to both

flocculation and coalescence. When dispersed in the presence of surfactant, coalescence was suggested to occur above a 1:1 oil/protein ratio. In our study, the spray-dried WPI sample was again used as a reference. After redispersing in water, a similar pattern to that of the redispersed emulsion was observed, suggesting that partial denaturation of protein in drying decreased the solubility of whey protein isolate. The solubility of the major whey proteins, β -lactoglobulin and α -lactalbumin, has been recently determined as a function of the outlet temperature of the spray dryer (27). An increase in the insoluble fraction was found above 80 $^{\circ}\text{C}$ for both proteins, representing approximately 5% of the total in both proteins at 90 $^{\circ}\text{C}$ with 20% solids in feed.

Physical Properties of the WPI Matrix. To determine the physical state of the matrix during the storage test, an attempt to determine the glass transition temperature (T_g) was made for the high humidity WPI reference sample (without oil), which was the most plasticized with water. At RH 91%, a weak baseline shift was found at 105 ± 1 $^{\circ}\text{C}$ (Figure 3). One of the difficulties in the determination of the glass transition temperature in globular proteins is that thermal denaturation, which occurs during the first heating (upper curves, Figure 3), changes protein structure (28). According to Sochava (28), release of water occurs in protein denaturation, which is likely to plasticize the protein further in the second heating. The baseline shift would have indicated that the samples were in a glassy state at 37 $^{\circ}\text{C}$ of the storage test. However, caking of the powder was observed at this humidity. To visualize the caking, the reference WPI powder (without oil) was imaged after 1 week storage at RH 91%. As expected, liquid bridging and coalescence of particles were observed (Figure 4A). Comparison of the inner structures of the dry powder (Figure 1B) with the powder stored at humid conditions (Figure 4B) revealed an enormous difference. A structural reorganization leading to aggregation had taken place during storage. This could reflect the nature of the partially denatured protein with exposed hydrophobic residues due to unfolding, which would act as a driving force for aggregation with increasing water content.

Oxidative Stability of Oil Emulsified in WPI Matrix and Bulk Oil. Oxidation of flaxseed oil was studied in the WPI matrix at 37 $^{\circ}\text{C}$ and at RH 0–91% using bulk oil as a reference. The initial rate of oxidation in bulk oils was very similar irrespective of the humidity (Figure 5), but after 9 weeks of storage (Figure 6), the amount of hydroperoxides in bulk oil was lowest at the intermediate humidity (RH 49%), a result similar to that obtained earlier for sea buckthorn oil (6), which is also rich in polyunsaturated fatty acids. Hydroperoxide contents at low humidities (RH 0% and RH 11%) were significantly higher ($P < 0.05$). In all cases, the rate of oxidation was essentially the same in bulk and matrix-dispersed oils for the first 3 weeks of storage. After this initial phase, oxidation occurred more rapidly in bulk oils. In all WPI samples, the amount of fatty acid hydroperoxides decreased after the initial phase and started to increase again after 5 weeks of storage. For the sample stored at RH 75%, lag time was even longer. Decrease in hydroperoxide content is possible due to the fact that hydroperoxides are not only formed but also simultaneously decomposing in oxidation (29). At the end of the storage test, oxidation had proceeded most in the dry sample (RH 0%). A minimum rate of oxidation was found at RH 75%, with no significant difference ($P > 0.05$) to the samples stored at RH 11% and RH 49%. Comparison of the bulk oil oxidation rate to the oxidation rate in the matrix-dispersed oil is not straightforward, since the surface area of dispersed oil is much higher, but on the other hand, oxygen concentration in the oil interface is likely to be reduced in the solid–liquid interface from that of the gas–liquid interface. The initial oxidation in the matrices

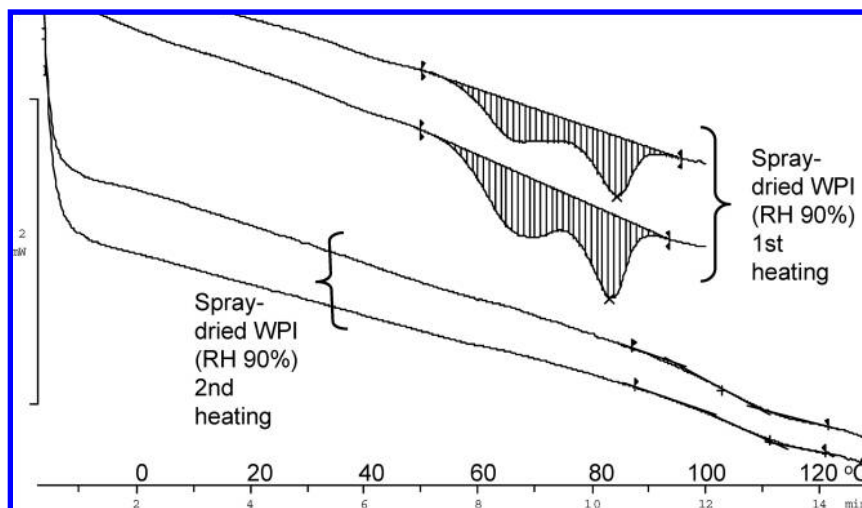


Figure 3. DSC curves on heating of duplicate WPI samples, denaturation on the first heating above, below the weak baseline transition in the second heating, which may be linked to glass transition of the protein matrix.

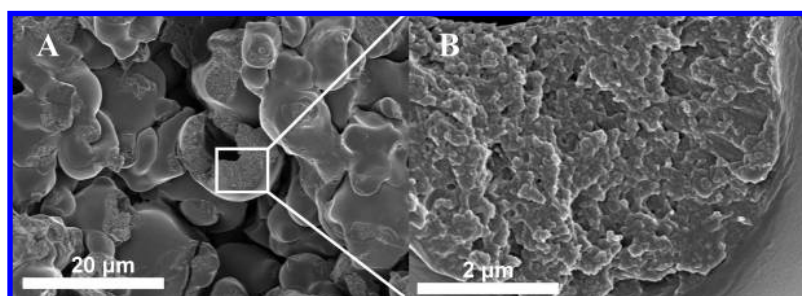


Figure 4. SEM micrograph of (A) spray-dried WPI powder (overview of torn surface, without oil) and of (B) cross-section of spray-dried WPI particle (without oil) after one week storage at RH 91% and 37 °C.

did not seem to be limited by oxygen concentration, which would suggest the role of oil in direct contact with air. There are two surfaces in these hollow sphere particles, of which the composition of the outer surface has been a subject of discussion previously. Baik et al. (9) observed a 10-fold increase in fish oil hydroperoxides in the surface oil compared to the encapsulated oil during the first days of storage. The role of surface oil in the initial rate of oxidation has also been suggested by Drusch et al. (30). In our study, the matrix was composed of surface-active protein, which was shown by ESCA to concentrate on the surface in drying. The powder particles in our study were extremely thin-walled (**Figure 1**), leaving a large vacuole with a possible oxygen reservoir inside.

Our results are in agreement with the well-known stability map by Labuza et al. (31), which suggests a high rate of oxidation at low and high humidities. However, divergence from the monolayer moisture stability (32) was found in the present study as the highest oxidative stability in the WPI matrix was found at RH 75%, which is expected to be well above monolayer moisture content. A deviation from monolayer stability was also recently reported for real food systems by Jensen and Risbo (33), who studied oxidative stability of peanuts, pork scratchings, and a mixture of rolled oats and wheat from muesli and oatmeal. Stapelfeldt et al. (34) studied oxidative stability of whole milk powder. The authors associated better stability with exposure to more heat in processing. The initial amount of reactive SH groups was found to be higher in the samples, which were less susceptible to oxidation, but the reduction in storage was the same for all of the samples. More recently, Thomsen et al. (35) have shown decoupling of the lipid oxidation rate from the rates of lactose crystallization, browning, and formation of radical species. According to Orlien, Risbo, Rantanen, and Skibstead

(36), hydroperoxide formation in glassy food matrices is controlled by different factors depending on temperature. At low temperatures (5 °C), the reaction rate and thus the oxygen consumption rate is slow, and the availability of oxygen is not rate limiting. At intermediate (25 °C) and high (up to 60 °C) temperatures, oxygen permeability becomes the rate determining factor in formation of lipid hydroperoxides. Permeability is affected by solubility and diffusion of gas in the matrix (3). As water plasticizes hydrophilic macromolecules, the increase in matrix molecular mobility is likely to increase diffusion within the matrix. Also, solubility of oxygen may be influenced by an increase in water content. Whitcombe et al. (3) reported a decrease in oxygen solubility in sugar alcohols with decreasing water content. The authors found that, with linear extrapolation, oxygen would be insoluble to sugar alcohols below 30% water content.

In the protein matrix of the present study, the absence of water did not decrease the rate of oxidation. Instead, the oxidation rate was highest in the conditions where little water was present (RH 0%). In terms of oxygen transport, this behavior could be interpreted as formation of cracks due to extreme drying (**Figure 7**). These cracks, if formed, were below resolution of SEM. Respectively, the structural reorganization observed in the protein matrix at high humidity (RH 91%) may be linked with the increased oxidation rate from RH 75% to RH 91%. According to Sundaresan and Ludescher (19), oxygen permeation in amorphous β -lactoglobulin films increased with the softening in the protein matrix in transition from a glassy to rubbery state. Our results were, however, unable to reliably show a glass transition in the protein matrix, despite the caking observed. Globular proteins are very compact structures suggesting that gas transport could be more efficient in the space

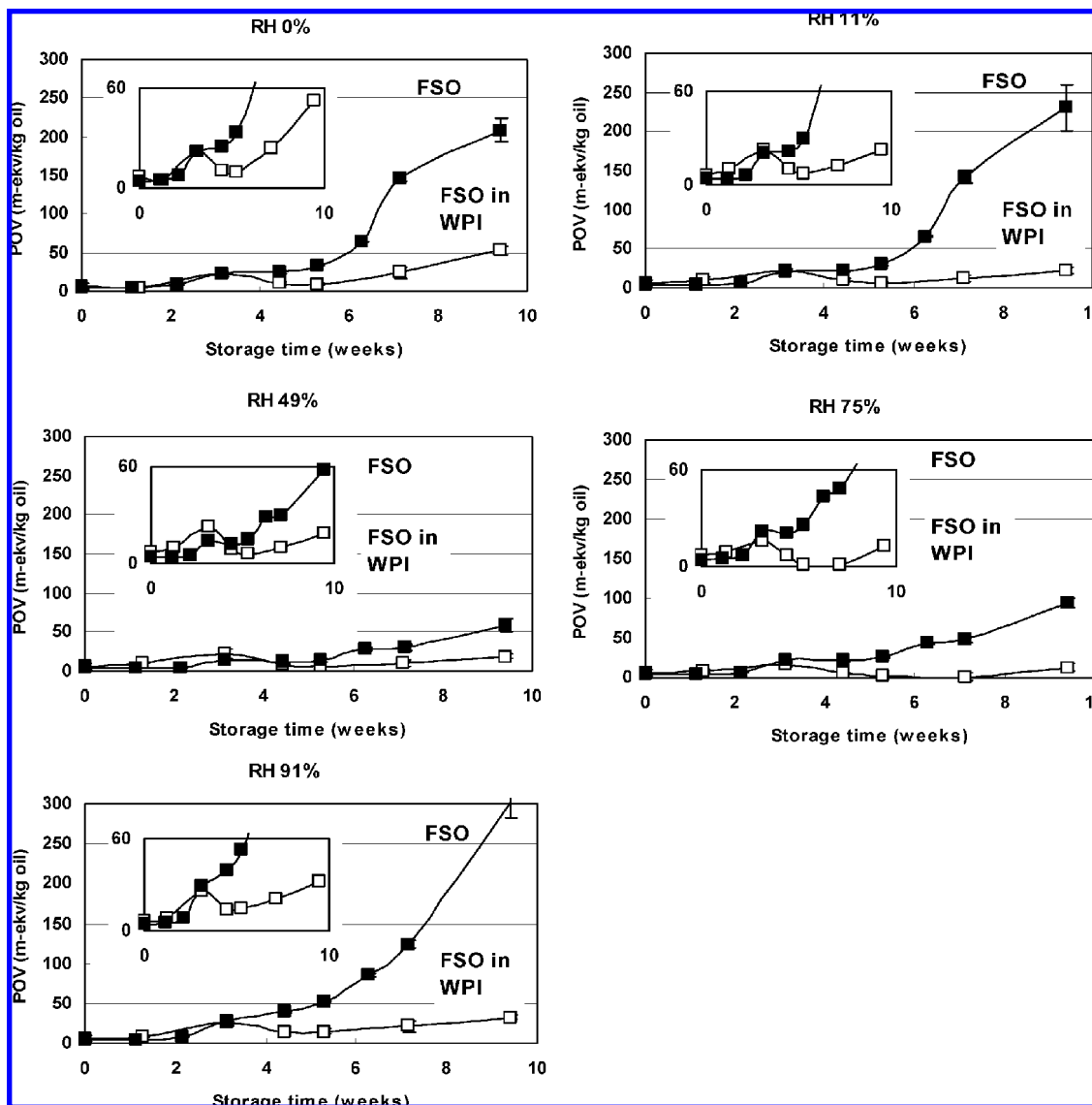


Figure 5. Oxidation of flaxseed oil (FSO) at 37 °C and RH 0–91% in WPI matrix and in bulk oil. Standard deviations are shown in error bars.

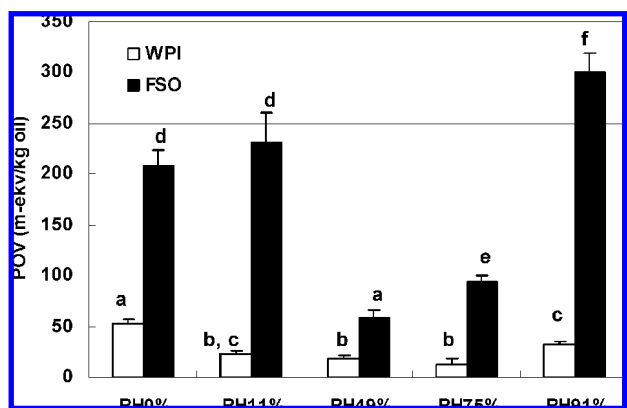


Figure 6. Peroxide values of bulk and spray-dried whey protein isolate emulsion of flaxseed oil after 9 weeks storage at 37 °C. Standard deviations are shown in error bars. Columns marked by same letter are not statistically different at $P < 0.05$.

between the globules. Aggregation of the globules at high humidity conditions is expected to reorganize the “cavities” in the matrix (Figure 7). The effect of the structural rearrangement of protein on oxidation rate was, however, minor as compared to the effect of crystallization of low-molecular-weight carbo-

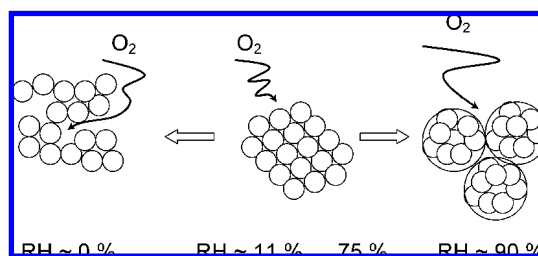


Figure 7. Schematic representation of the effect of water on oxygen transport in the matrix of a globular protein. Structural changes occur at extreme cases, both with the elimination of water and with saturation (close to) with water. At extremely dry conditions, cracking of the matrix would facilitate oxygen transport and explain the observed high rate of oxidation. At high humidity conditions, the observed formation of aggregates may create cavities for oxygen transport.

hydrates associated with matrix collapse and oil release (30, 37). This may suggest the importance of the interfacial layer in controlling gas permeation, as suggested by Moreau and Rosenberg (18). The very low rate of oxidation at RH 75% could not be explained by the results of the present study. Partial heat denaturation of matrix proteins could increase antioxidant capacity by exposure of buried thiol groups in protein as well as breakage of

disulfide bridges. Also, the amount of free radicals has been shown to decrease with increasing humidity from RH 30% to RH 65% in various protein-containing matrices (33). The suggested water-related factors involved in the rate of oil oxidation in the protein matrix are summarized in **Figure 7**.

In conclusion, the WPI matrix retarded flaxseed oil oxidation from that of bulk oil. The rate of flaxseed oil oxidation in the matrix was increased by low and high environmental humidity. In addition to visually observed caking, SEM revealed changes in the internal structure of the matrix at high humidity. The effect of humidity on oxidation in the powder matrix might be explained by the increasing reactivity of the protein with increasing humidity.

ACKNOWLEDGMENT

Anne Ala-Kahrakuusi, Jaana Lehtinen, and Liisa Änäkäinen are acknowledged for their skilful technical assistance. The authors thank Mikael Sundin for performing the ESCA analysis.

LITERATURE CITED

- Coupland, J.; McClements, D. Lipid oxidation in food emulsions. *Trends Food Sci. Technol.* **1996**, *7*, 83–91.
- McClements, D.; Decker, E. Lipid oxidation in oil-in-water emulsions: impact of molecular environment on chemical reactions in heterogeneous food systems. *J. Food Sci.* **2000**, *65*, 1270–1282.
- Whitcombe, M.; Parker, R.; Ring, S. Oxygen solubility and permeability of carbohydrates. *Carbohydr. Res.* **2005**, *340*, 1523–1527.
- Stading, M.; Rindlav-Westling, A.; Gatenholm, P. Humidity-induced structural transitions in amylose and amylopectin films. *Carbohydr. Polym.* **2001**, *45*, 209–217.
- Forsell, P.; Lahtinen, R.; Lahelin, M.; Myllärinen, P. Oxygen permeability of amylose and amylopectin films. *Carbohydr. Polym.* **2002**, *47*, 125–129.
- Partanen, R.; Hakala, P.; Sjövall, O.; Kallio, H.; Forsell, P. Effect of relative humidity on the oxidative stability of microencapsulated sea buckthorn seed oil. *J. Food Sci.* **2005**, *70*, E37–E43.
- Sootitiantawat, A.; Yoshii, H.; Furuta, T.; Ohgawara, M.; Forsell, P.; Partanen, R.; Poutanen, K.; Linko, P. Effect of water activity on the release characteristics and oxidative stability of D-limonene encapsulated by spray drying. *J. Agric. Food Chem.* **2004**, *52*, 1269–1276.
- Hardas, N.; Danviriyakul, S.; Foley, J.; Nawar, W.; Chinachoti, P. Effect of relative humidity on the oxidative and physical stability of encapsulated milk fat. *JAOCs* **2002**, *79*, 151–158.
- Baik, M.-Y.; Suhendro, E.; Nawar, W.; McClements, D.; Decker, E.; Chinachoti, P. Effects of antioxidants and humidity on the oxidative stability of microencapsulated fish oil. *J. Am. Oil Chem. Soc.* **2004**, *81*, 355–360.
- Kagami, Y.; Sugimura, S.; Fujishima, N.; Matsuda, K.; Kometani, T.; Matsumura, Y. Oxidative stability, structure and physical characteristics of microcapsules formed by spray drying of fish oil with protein and dextrin wall materials. *J. Food Sci.* **2003**, *68*, 2248–2255.
- Keogh, M.; O’Kennedy, B.; Kelly, J.; Auty, M.; Kelly, P.; Fureby, A.; Haahr, A.-M. Stability to oxidation of spray-dried fish oil powder microencapsulated using milk ingredients. *J. Food Sci.* **2001**, *66*, 217–224.
- Stapelheldt, H.; Nielsen, B.; Skibsted, L. Effect of heat treatment, water activity and storage temperature on the oxidative stability of whole milk powder. *Int. Dairy J.* **1997**, *7*, 331–339.
- McHugh, T.; Krochta, J. Sorbitol- vs glycerol-plasticised whey protein edible films: integrated oxygen permeability and tensile property evaluation. *J. Agric. Food Chem.* **1994**, *42*, 841–845.
- Maté, J.; Krochta, J. Comparison of oxygen and water vapour permeabilities of whey protein isolate and β -lactoglobulin films. *J. Agric. Food Chem.* **1996**, *44*, 3001–3004.
- Sothornvit, R.; Krochta, J. Oxygen permeability and mechanical properties of films from hydrolysed whey protein. *J. Agric. Food Chem.* **2000**, *48*, 3913–3916.
- Hong, S.-I.; Krochta, J. Oxygen barrier performance of whey-protein-coated plastic films as affected by temperature, relative humidity, base film and protein type. *J. Food Eng.* **2006**, *77*, 739–745.
- Moreau, D.; Rosenberg, M. Oxidative stability of anhydrous milkfat microencapsulated in whey proteins. *J. Food Sci.* **1996**, *61*, 39–43.
- Moreau, D.; Rosenberg, M. Porosity of whey-protein based microcapsules containing anhydrous milkfat measured by gas displacement pycnometry. *J. Food Sci.* **1998**, *63*, 819–823.
- Sundaresan, K.; Ludescher, R. Molecular mobility and oxygen permeability in amorphous β -lactoglobulin films. *Food Hydrocolloids* **2008**, *22*, 403–413.
- Kellerby, S.; McClements, D.; Decker, E. Role of proteins in oil-in-water emulsions on the stability of lipid hydroperoxides. *J. Agric. Food Chem.* **2006**, *54*, 7879–7884.
- International Dairy Federation. International IDF Standards, Section 74A, 2005.
- Fäldt, P.; Bergenstahl, B.; Carlsson, G. The surface coverage of fat on food powders analysed by ESCA (electron spectroscopy for chemical analysis). *Food Struct.* **1993**, *12*, 225–234.
- Ré, M. Microencapsulation by spray-drying. *Drying Technol.* **1998**, *16*, 1195–1236.
- Wooster, T.; Augustin, M. β -Lactoglobulin-dextran Maillard conjugates: their effect on interfacial thickness and emulsion stability. *J. Colloid Interface Sci.* **2006**, *303*, 564–572.
- Millqvist-Fureby, A.; Elofsson, U.; Bergenstahl, B. Surface composition of spray-dried milk protein-stabilised emulsions in relation to pre-heat treatment of proteins. *Colloids Surf., B* **2001**, *21*, 47–58.
- Hogan, S.; McNamee, B.; O’Riordan, E.; O’Sullivan, M. Microencapsulating properties of whey protein concentrate 75. *J. Food Sci.* **2001**, *66*, 675–680.
- Anandharamakrishnan, C.; Rielly, C.; Stapley, A. Loss of solubility of α -lactalbumin and β -lactoglobulin during the spray drying of whey proteins. *LWT—Food Sci. Technol.* **2008**, *41*, 270–277.
- Sochava, I. Heat capacity and thermodynamic characteristics of denaturation and glass transition of hydrated and anhydrous protein. *Biophys. Chem.* **1997**, *69*, 31–41.
- Fritch, C. Lipid oxidation—the other dimensions. *Int. News Fats, Oils Relat. Mater.* **1994**, *5*, 423–436.
- Drusch, S.; Serfert, Y.; Van Den Heuvel, A.; Schwarz, K. Physicochemical characterization and oxidative stability of fish oil encapsulated in an amorphous matrix containing trehalose. *Food Res. Int.* **2006**, *39*, 807–815.
- Labuza, T. Kinetics of lipid oxidation in foods. *CRC Rev. Food Technol.* **1971**, *2*, 335–405.
- Labuza, T. The effect of water activity on reaction kinetics of food deterioration. *Food Tech.* **1980**, *34* (4), 36–41, 59.
- Jensen, P.; Risbo, J. Oxidative stability of snack and cereal products in relation to moisture sorption. *Food Chem.* **2007**, *103*, 717–724.
- Stapelheldt, H.; Nielsen, B.; Skibsted, L. Effect of temperature, water activity and storage temperature on the oxidative stability of whole milk powder. *Int. Dairy J.* **1997**, *7*, 331–339.
- Thomsen, M.; Lauridsen, L.; Skibsted, L.; Risbo, J. Two types of radicals in whole milk powder. Effect of lactose crystallization, lipid oxidation and browning reactions. *J. Agric. Food Chem.* **2005**, *53*, 1805–1811.
- Orlien, V.; Risbo, J.; Rantanen, H.; Skibsted, L. Temperature-dependence of rate of oxidation of rapeseed oil encapsulated in a glassy food matrix. *Food Chem.* **2006**, *94*, 37–46.
- Labrousse, S.; Roos, Y.; Karel, M. Collapse and crystallization in amorphous matrices with encapsulated compounds. *Sci. Aliments* **1992**, *12*, 757–769.

Received for review February 26, 2008. Revised manuscript received April 30, 2008. Accepted May 8, 2008. The work was carried out in TAINA project belonging to the FinnNano technology program run by the Finnish Funding Agency for Technology and Innovation (Tekes).